Sensors & Actuators: B. Chemical 301 (2019) 127120

Contents lists available at ScienceDirect

Sensors and Actuators B: Chemical

journal homepage: www.elsevier.com/locate/snb

Layer-by-layer assembly of polyelectrolytes-wrapped multi-walled carbon nanotubes on long period fiber grating sensors

Yi-Qing Ni[a,*], Siqi Ding[a], Baoguo Han[b], Huaping Wang[a,c]

[a] Department of Civil and Environmental Engineering, The Hong Kong Polytechnic University, Hung Hom, Kowloon, Hong Kong, China
[b] School of Civil Engineering, Dalian University of Technology, Dalian 116024, China
[c] School of Civil Engineering and Mechanics, Lanzhou University, Lanzhou 730000, China

ARTICLE INFO

Keywords:
Long period fiber grating
Sensor
Carbon nanotube
Layer-By-Layer assembly
Thin film
pH sensing

ABSTRACT

A new type of long period fiber grating (LPG) sensor coated with polyelectrolytes-wrapped multi-walled carbon nanotube (MWCNT) (PE-CNT) thin film is reported in this study. The novel nanostructured thin film is deposited on the LPG grating region using a layer-by-layer assembly technique. The aim of using polyelectrolytes (PE) including poly(ethylenimine) (PEI) and poly(acrylic acid) (PAA) in the coating layer is to improve the dispersion of MWCNTs and to enhance the adhesion of functionalized MWCNTs on the LPG surface. The structures and morphologies of the MWCNT-based nanostructured thin film are observed by scanning electron microscopy characterization. The refractive index and pH sensing behaviors of LPGs with pure $(PE)_{10}$ thin film and with $(PE\text{-}CNT)_{10}$ thin film, respectively are compared. Results show that for LPG with $(PE\text{-}CNT)_{10}$ thin film the transmission intensity at the resonance wavelength decreases noticeably with the increase of the surrounding refractive index. This is distinct from the sensing mechanism of LPG with $(PE)_{10}$ thin film, which is based on the resonance wavelength shift. The LPG with a $(PE\text{-}CNT)_{10}$ thin film provides enhanced pH sensitivity compared with that of a $(PE)_{10}$ thin film. The LPG with $(PE\text{-}CNT)_{10}$ thin film has a fast response rate and a good repeatability, thus demonstrating its strong potentiality for practical monitoring applications.

1. Introduction

Mechanical stresses and chemical attacks are the two main causes for the deterioration in public infrastructure, especially in coastal and marine reinforced concrete structures. It is of importance to monitor the long-term performance of concrete structures in aggressive environments with the intention of understanding the evolutionary deterioration mechanism. This requires the development of durable, embeddable and multi-functional sensors for multi-scale and multi-physics monitoring [1–3].

Since the first engraving on optical fibers in 1996, there has been increasing interest of research in the use of long period fiber grating (LPG) sensors for temperature, strain and curvature measurements owing to their attractive merits such as stable operation in hazardous environments, immunity to electromagnetic radiation, remotely real-time monitoring, low cost and small size [4]. LPG consists of a periodic modulation in the refractive index of the fiber core with its grating wavelength ranging from tens to several hundred micrometers, in which light coupling occurs between the fundamental core mode and the forward co-propagating cladding modes at discrete wavelengths, thus generating several attenuation bands in the transmission spectrum. The phase matching condition is given by

$$\lambda_{res} = (n_{co}^{eff} - n_{cl,m}^{eff})\Lambda \quad (1)$$

where λ_{res} is the resonant wavelength due to the coupling; n_{co}^{eff} and $n_{cl,m}^{eff}$ are the effective refractive indices of the core mode and the mth cladding mode, respectively; and Λ is the grating period [5]. Due to the high dependence of the effective refractive index of the cladding modes on the refractive index of the surrounding environment, LPG is ultra-sensitive to the refractive index change of the medium surrounding the cladding by detecting the variation in resonance wavelength of the attenuation bands [6]. This sensitivity of LPG to the surrounding refractive index can be further enhanced by depositing a thin film with high refractive index on the cladding region. It has been theoretically verified that the thin film enables a transition in which cladding guided modes are coupled to the thin film guided mode causing a strong reorganization of the cladding mode and increasing the intensity of the evanescent field at the interface between the layer and the surrounding medium [7]. In other words, a change in refractive index or thickness of the thin film can induce the wavelength shift and amplitude variation of

* Corresponding author.
E-mail address: ceyqni@polyu.edu.hk (Y.-Q. Ni).

https://doi.org/10.1016/j.snb.2019.127120
Received 2 January 2018; Received in revised form 6 September 2019; Accepted 9 September 2019
Available online 12 September 2019

the attenuation bands. In this connection research has developed in the past decade on the use of LPGs coated with sensitive thin films for biological, chemical and environmental sensing by means of the detection of refractive index change. In particular, the advancement of nanotechnology has realized the integration of nanostructured materials with LPG sensors. Nanostructured coatings offer unique properties that lead to the development of novel optical fiber sensors [8].

Carbon nanotubes (CNTs) are allotropes of carbon with a hollowly cylindrical nanostructure. They are generally a few nanometers in diameter and several microns in length. According to the number of rolled layers of graphene, CNTs are categorized as single-walled CNTs (SWCNTs) and multi-walled CNTs (MWCNTs) [9]. Due to their hollow structures with a very large surface area and aspect ratio, unique physical properties and stable chemical and mechanical properties, CNTs, especially MWCNTs, have been viewed as one of the most promising thin film materials for the design of biological and chemical sensors. In fact, the unique morphology of CNTs offers them a superior function to reversibly adsorb molecules of various target species by the mechanism of modulation of their electrical, optical and geometrical properties, such as resistivity, dielectric constant and thickness [10,11]. In addition, CNTs have been successfully deposited as thin films on the surface of optical fibers for a wide range of sensing applications [12–16]. Therefore, CNT-based LPG sensors offer the possibility of excellent sensitivity, stable operating condition, rapid response rate and being sensitive to various kinds of chemicals [17].

However, the solid adhesion of CNTs on the LPG surface is still a challenging issue when considered for practical applications in aggressive environments. Moreover, the realization of CNT thin films with a controllable thickness is an important basis for the optimization of sensing performance of their final devices [18]. Tan et al. [13] employed a mechanical spray coating method to coat a CNT thin film on the grating region of LPG sensor. The spray coating method is considered as a relatively fast, simple and cost-effective deposition method [19]. However, with this technique it is difficult to control the architecture of CNT thin films at the nanometer and micrometer scale. Furthermore, homogeneity cannot be guaranteed. Consales et al. [11] deposited cadmium arachidate (CdA)/SWCNT composites thin film upon the distal end of standard single-mode fibers by the Langmuir-Blodgett deposition technique. The CdA matrix used as linker–buffer material which affords a better adhesion of the CNTs to the fiber optic surface. The Langmuir–Blodgett deposition technique enables a precise control of the layer thickness at the molecular level and can be used for deposition on almost any kind of solid substrate [20]. However, it requires specialized equipment, as well as careful cleaning and preparation of the substrate. In addition, the Langmuir–Blodgett technique cannot be used to form films thicker than several monolayers. The low speed of the deposition procedure as well as the limited number of materials suitable for this technique have restricted its extensive utilization in the field of nanostructured thin film assembly [21]. A simple approach to assemble dispersed CNTs into thin films is using a layer-by-layer (LBL) assembly, which consists of the repeated, sequential immersion of a substrate into a polyanion and polycation material respectively. This technique can control the thickness of thin films at the nanometer scale, thus precisely tailoring film properties and functionality [22]. While this novel deposition technique has been applied for fabrication of diverse polyelectrolyte systems onto optical fiber sensors, such as PDDA/PSS [7], PAA/PAH [23,24], Al_2O_3/PSS [24] and PEI/PAA [25,26], the capability of CNT thin films integrated on LPG sensors has been seldom reported.

In this study, we exploit the LBL assembly technique to deposit MWCNT thin film on LPG sensors for the first time to the best of our knowledge. MWCNTs functionalized with carboxylic acid groups and MWCNTs functionalized with amine groups are treated as negatively-charged and positively-charged components, respectively. In order to strengthen the adhesion of functionalized MWCNTs on the LPG surface, the two kinds of MWCNTs are wrapped with weak polyelectrolytes including poly(ethylenimine) (PEI) and poly(acrylic acid) (PAA). It is worth noting that MWCNTs are inherently hydrophobic and easy to agglomerate due to their van der Waals interactions. The noncovalent functionalization has been reported as an effective method to obtain homogeneous and stable CNTs dispersions in water by using PEI or PAA polymer [27–29]. This mechanism is motivated by a thermodynamic drive to remove the hydrophobic interface between the CNTs and the polymer solutions [30]. In such a manner, a stable and uniform polyelectrolytes-wrapped MWCNTs thin film is coated on the LPG surface. For comparison, a LPG coated with a pure PEI/PAA thin film is also fabricated using LBL assembly. The performance of the two sensors for refractive index and pH sensing is then compared.

2. Experiment

2.1. Materials

Polyelectrolytes. Branched poly(ethylenimine) (PEI) (Aldrich, Mw ~ 750,000 g/mol, 50 wt.% aqueous solution) is chosen as the polyanion and diluted with ultrapure water to a concentration of 2 mg/ml, where the pH of PEI solution is adjusted to pH 11.0 by adding 1.0 M sodium hydroxide (NaOH). Poly(acrylic acid) (PAA) (Aldrich, Mw ~ 450,000 g/mol) is selected as the polycation and also dissolved to 2.0 mg/ml, where the pH of PAA solution is calibrated to a pH 3.0 value by adding 1.0 M hydrochloric acid (HCl). All the chemicals are reagent grade and used without further purification.

Negatively and positively charged MWCNTs. Carboxylic acid functionalized MWCNTs (MWCNT-COOH, 95% purity, length 0.5–2 μm, outer diameter 8–15 nm) and amine functionalized MWCNTs (MWCNT-NH_2, 95% purity, length 0.5–2 μm, outer diameter 8–15 nm) are used in this study. Both MWCNT-COOH and MWCNT-NH_2 powders are filtered and washed with ultrapure water (18 MΩ·cm, Barnstead, Smart2Pure) three times and dried at 55°C in vacuum for 24 h prior to use. Dried MWCNT-COOH and MWCNT-NH_2 powders are uniformly dispersed in ultrapure water with a concentration of 0.2 mg/ml and sonicated using an ultrasonic cleaner (Crest, 45 kHz) for 1 h.

Polyelectrolytes-wrapped MWCNTs. PAA powder is added into the above well-dispersed MWCNT-COOH solution (0.2 mg/ml in ultrapure water) to create a PAA-CNT solution with a concentration of 2 mg/ml. Similarly, a positively charged PEI solution is added into a MWCNT-NH_2 solution (0.2 mg/ml in ultrapure water) to create a PEI-CNT solution with a concentration of 2 mg/ml. The PAA-CNT and PEI-CNT solutions are sonicated for 0.5 h prior to a LBL assembly. Fig. 1(a) illustrates the synthetic process of MWCNTs wrapped with PAA and PEI polymers. After functionalization, positively charged PEI-CNT and negatively charged PAA-CNT are obtained for the LBL assembly. The stabilized dispersion of noncovalent functionalized CNTs in the two polymer solutions can be achieved for a long time, as demonstrated in Fig. 1(b).

2.2. Layer-by-layer assembly of thin films

The LBL assembly of oppositely charged polyelectrolytes (positively charged PEI or PEI-CNT and negatively charged PAA or PAA-CNT) is made on silicon wafers for characterization and then induced on LPGs (with a length of 20 mm and a grating period of 550 μm) for testing. The substrates are piranha-treated with 7:3 of concentrated sulfuric acid (H_2SO_4) and 30% hydrogen peroxide (H_2O_2) for 20 min at 100 °C, washed with ultrapure water for several times and then rinsed with ultrapure water before use. The negatively charged substrate is dried with nitrogen and first immersed into positively charged PEI or PEI-CNT solutions for 15 min, followed by rinsing with ultrapure water for 2 min. The substrate is then exposed to negatively charged PAA or PAA-CNT solutions for 15 min and washed with ultrapure water for 2 min. This cycle forms one bilayer of oppositely charged polyelectrolytes, named as $(PEI/PAA)_1$ or $(PEI\text{-}CNT/PAA\text{-}CNT)_1$. The same cycle is

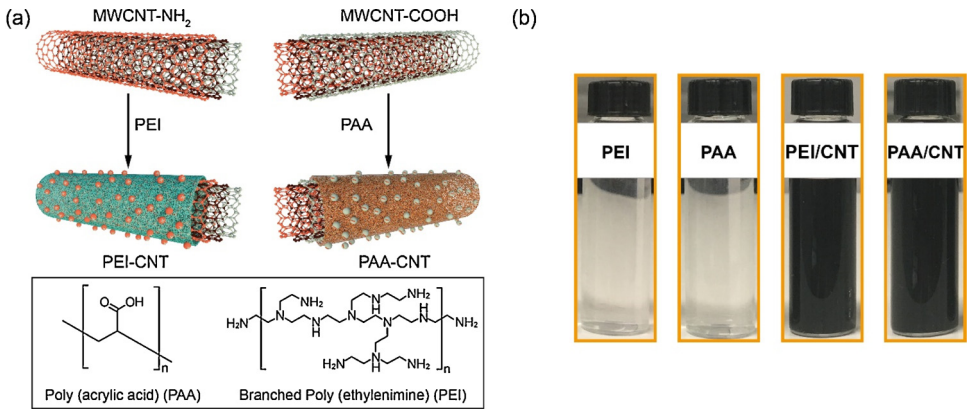

Fig. 1. (a) Schematic of the synthetic process of MWCNTs wrapped with PAA and PEI polymers and the chemical structures of PAA and PEI; (b) Pictures of PEI, PAA, PEI-CNT and PAA-CNT solutions maintained for about 4 months.

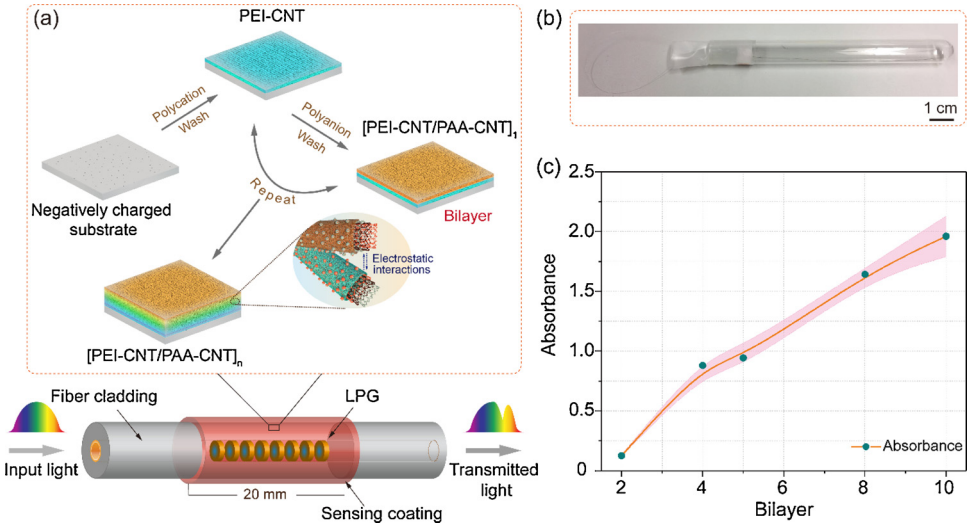

Fig. 2. (a) Layer-by-layer (LBL) assembled thin film with positively charged PEI-CNT and negatively charged PAA-CNT via electrostatic interaction; (b) As-made LPG sensor encapsulated in a test tube; (c) UV absorbance at 260 nm as a function of the bilayer number.

repeated to reach the desired number of bilayers. The substrate is then annealed for 12 h at 80 °C before testing. The schematic illustration of the LBL assembly of PEI-CNT/PAA-CNT films is shown in Fig. 2(a). All films described here consist of 10 bilayers, i.e. $(PEI/PAA)_{10}$ or $(PEI\text{-}CNT/PAA\text{-}CNT)_{10}$. Fig. 2(b) shows a photo of LPG coated with $(PEI\text{-}CNT/PAA\text{-}CNT)_{10}$ thin film encapsulated in a test tube. For the sake of brevity, $(PEI/PAA)_{10}$ and $(PEI\text{-}CNT/PAA\text{-}CNT)_{10}$ are simply denoted as $(PE)_{10}$ and $(PE\text{-}CNT)_{10}$ respectively in the following sections.

2.3. Characterization

The morphological characterization of the thin films is carried out by a scanning electron microscopy (SEM, Tescan VEGA3) with an accelerating voltage of 20 kV. The LBL assembly process of the $(PE\text{-}CNT)_{10}$ thin film is monitored with a UV–vis spectrophotometer (MRC, Spectro UV-11). As shown in Fig. 2(c), the absorbance at 260 nm increases with an increasing bilayer number of the thin films, indicating that the PE-CNT multilayers can grow steadily and have a good assembling feature to form thin films on the LPG surface. For optical characterization, the LPG is fixed using two fiber holders in order to eliminate mechanical bending. The transmission spectrum is monitored by connecting one end of the LPG sensor to a broadband light source (Amonics SLD) and the other to an optical spectrum analyzer (OSA, YOKAGAWA AQ6370) with a resolution of 0.02 nm. A refractive index sensing test is then conducted by placing the grating region of the LPG sensor in a Teflon V groove, which is filled with a set of refractive index solutions ranging from 1.34 to 1.44. The refractive index solutions are prepared by diluting various concentrations of glycerin with ultrapure water, with the refractive index of each solution being calibrated with a digital refractometer (Reichert AR200) with a resolution of 0.0001. After each measurement, both the LPG sensors and the groove are washed with ultrapure water in order to avoid contamination to the next refractive index solution. All the measurements are conducted at a constant environmental temperature of 23 ± 0.5 °C.

3. Results and discussion

3.1. Morphology of $(PE)_{10}$ and $(PE\text{-}CNT)_{10}$ thin films

The morphology of the $(PE)_{10}$ and $(PE\text{-}CNT)_{10}$ thin films on silicon wafers is compared as shown in Fig. 3. Note that the surface structures of LBL thin films are not influenced by different shapes of the silicon substrates. This means that similar morphology can be observed in films either on silicon wafers or on LPG sensors. The $(PE)_{10}$ thin film exhibits remarkably smooth and uniform surface features (see Figs. 3(a) and (b)), which is a typical morphology of a PEI/PAA multilayer [31]. This indicates that the sensing film is well deposited by the LBL assembly technique. Differently, a $(PE\text{-}CNT)_{10}$ thin film provides a rough and speckled surface with isolated craterlike micron-scale pores (see Figs. 3(c) to (f)). A similar porous morphology is observed in a MWNT/

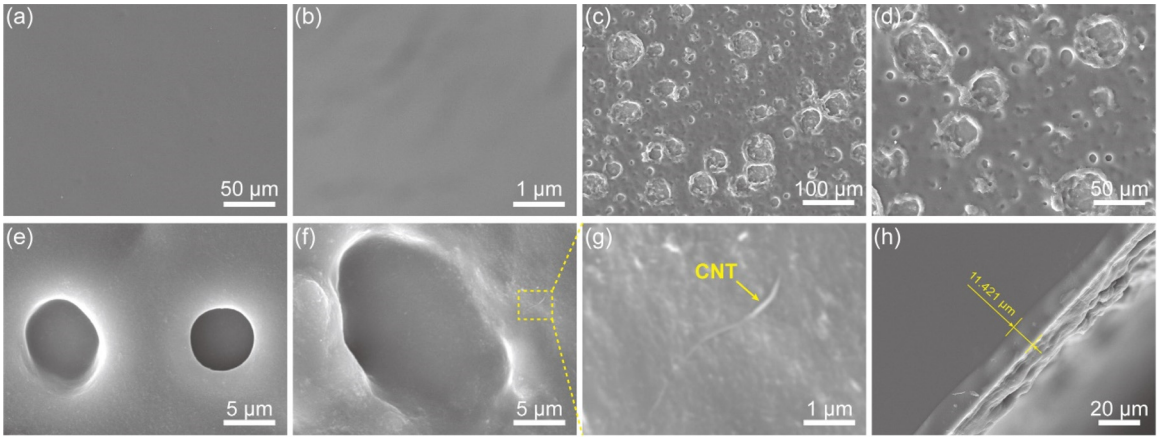

Fig. 3. Scanning electron microscopy (SEM) images of the $(PE)_{10}$ thin film: (a) 1000x, (b) 50000x; and of the $(PE\text{-}CNT)_{10}$ thin film: (c) 500x, (d) 1000x; (e) and (f) Craterlike micro-scale pores; (g) An enlarged view of one polyelectrolytes-wrapped MWCNT bundle; (h) A cross-section view of the $(PE\text{-}CNT)_{10}$ thin film on a silicon wafer.

QC-P4VP thin film due to the irregular shape of the CNTs [32]. This porous nature of a thin film facilitates the permeability retention of analytes, resulting in a high sensitivity with a simultaneously enhanced response rate of thin film-coated optical fiber sensors [33,34]. It is of great importance to enable the real-time measurement of chemical and biochemical sensing. Fig. 3(g) shows a SEM image of one MWCNT array, which has a wider diameter than the immaculate MWCNT, indicating polyelectrolytes wrapping around the MWCNTs [28]. The thickness of the $(PE\text{-}CNT)_{10}$ thin film is measured to be approximately 11.421 μm as shown in Fig. 3(h).

3.2. Optical characterization of thin film-coated LPG sensors

The deposition of high refractive index thin films onto LPG sensors induces a re-distribution of the cladding modes, i.e., a change in the effective refractive indices of the cladding modes leading to a wavelength and transmission intensity change for the attenuation bands [7]. Fig. 4 shows the measured transmission spectra of LPGs before and after coating with $(PE)_{10}$ and $(PE\text{-}CNT)_{10}$ thin films. As expected, all the LPGs exhibit blue shifts after applying thin films coatings. Also, a decrease in the transmission intensity of the resonance wavelength was observed for all the LPG sensors.

When the LPG with $(PE\text{-}CNT)_{10}$ thin film is immersed in glycerin solutions with the refractive index (RI) varying from 1.3488 to 1.4337,

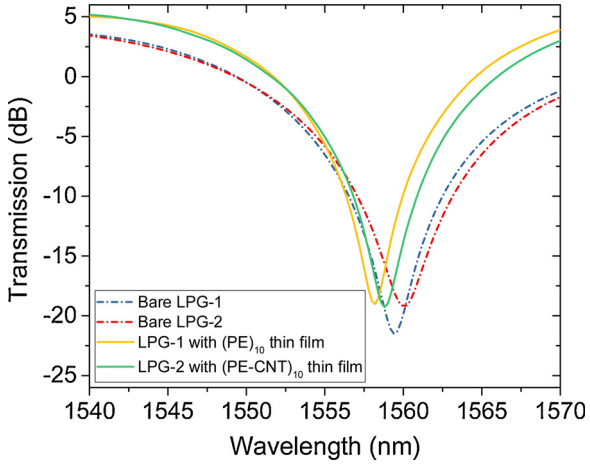

Fig. 4. Comparison between the transmission spectra of bare LPGs with air as external medium and LPGs with a $(PE)_{10}$ thin film (LPG-1) and with a $(PE\text{-}CNT)_{10}$ thin film (LPG-2).

the corresponding transmission spectra are shown in Fig. 5(a). It can be seen that there is little variation in the resonance wavelength of the attenuation bands, while the transmission intensity at resonance wavelength decreases with the increase of the RI of the external environment. There is no attenuation band that disappears as the external RI is less than the cladding index [6]. This behavior can be explained by the fact that a portion of propagating light of the cladding mode is reflected by the $(PE\text{-}CNT)_{10}$ thin film due to the high RI and high light absorbance of CNTs. The amount of reflectance at the interface between the cladding and the $(PE\text{-}CNT)_{10}$ thin film decreases as the external RI increases, which indicates that the intensity of evanescent waves is attenuated and thus causes a reduction in the transmission intensity of the attenuation band [13,35]. The variation of the resonance wavelength and the transmission intensity of the attenuation bands versus the RI of the external environment is shown in Fig. 5(b). The change of the transmission intensity as a function of the external RI tends to be nonlinear. In the 1.3488–1.4337 region, the total change in the transmission intensity is 7.214 dB, indicating that the average sensitivity is approximately 85 dB/RIU. This value is much higher than those of other optical fiber RI sensors reported in the literature [36,37]. It should be noted that the observed slight wavelength fluctuation around 1558 nm is likely due to measurement errors by the OSA and the light source and the differences during their operation. For comparison, we have also measured the transmission spectra of the LPG with a $(PE)_{10}$ thin film, which has a much lower RI and light absorbance than the $(PE\text{-}CNT)_{10}$ thin film. As shown in Figs. 6(a) and (b), the resonance wavelengths of this sensor, as expected, produce a substantial blue shift with increasing external RI ($\Delta\lambda \approx 3$nm), whereas the change in transmission intensity is relatively small compared with the LPG with $(PE\text{-}CNT)_{10}$ thin film. This means that LPGs coated with $(PE)_{10}$ thin film and with $(PE\text{-}CNT)_{10}$ thin film display totally different working mechanisms. The relationship between the transmission intensity at a wavelength of 1558 nm and the external RI of the LPG with a $(PE\text{-}CNT)_{10}$ thin film has the advantage of achieving intensity demodulation, which requires only a straightforward signal processing technique and provides real-time measurement of the analytes.

In order to evaluate the reliability of the LPG with $(PE\text{-}CNT)_{10}$ thin film, the sensor is exposed an increasing-decreasing RI variation from 1.3723 to 1.4337 as shown in Fig. 7(a). It is observed that the sensor maintains good stability with a maximum error of 0.61 dB. The relationship between the transmission intensity and the external RI can be approximately linearly expressed by $y = 103.873x - 158.998$. Fig. 7(b) shows the dynamic response of the fabricated RI sensor to four cycles at RI = 1.3488 and at RI = 1.4337. After several repeated tests, the transmission intensity of the sensor for a specified RH is nearly constant

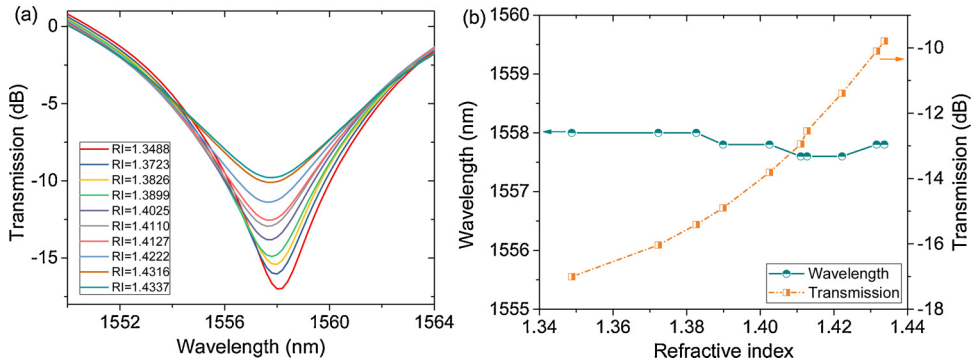

Fig. 5. (a) Transmission spectra of the LPG with $(PE\text{-}CNT)_{10}$ thin film exposed to glycerin solutions with the refractive index (RI) varying from 1.3488 to 1.4337; (b) Dependence of wavelength shift and transmission intensity change on the external refractive index.

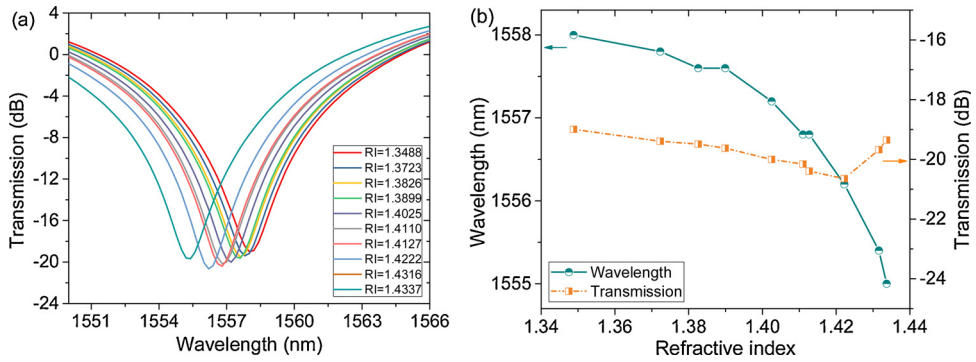

Fig. 6. (a) Transmission spectra of the LPG with $(PE)_{10}$ thin film exposed to glycerin solutions with the refractive index (RI) varying from 1.3488 to 1.4337; (b) Dependence of wavelength shift and transmission intensity change on the external refractive index.

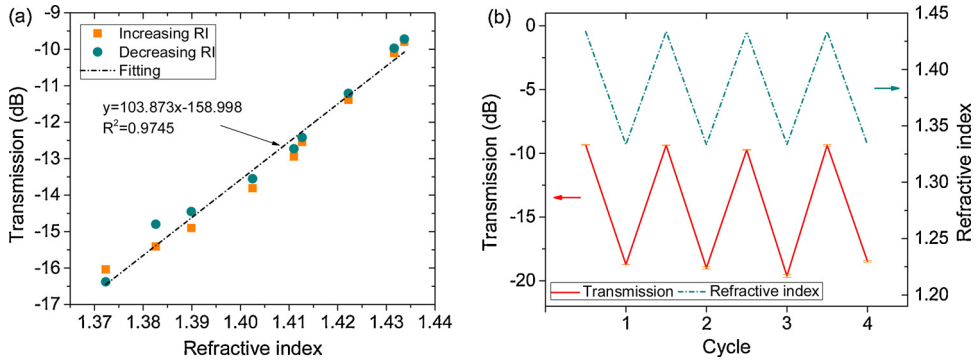

Fig. 7. (a) Relationship between the transmission intensity and the external refractive index (RI) of the LPG with $(PE\text{-}CNT)_{10}$ thin film; (b) Dynamic response of the LPG with $(PE\text{-}CNT)_{10}$ thin film to four cycles at RI = 1.3488 and at RI = 1.4337.

without significant degradation of sensitivity, implying that the fabricated LPG with $(PE\text{-}CNT)_{10}$ thin film has good repeatability and is suitable for the RI sensor. The solid adhesion of $(PE\text{-}CNT)_{10}$ thin film on the LPG surface via electrostatic interactions contributes to the favorable sensing performance of the sensor.

Furthermore, owing to the pH-dependent thickness behavior of polyelectrolytes, LPGs based on polyelectrolyte thin films have been studied to develop pH sensors [38–40]. In this paper, we also compare the performance of the LPG with $(PE\text{-}CNT)_{10}$ and $(PE)_{10}$ thin films in aqueous pH buffers for different pH between 2 and 13 as shown in Fig. 8. The pH measurements are conducted by the same method as the RI measurements discussed in Section 3.3. The values of RI of all the pH buffers for test are close to water, i.e. 1.3333. For the LPG with $(PE)_{10}$ thin film, its pH responses remain almost unchanged. Differently, with the addition of CNT into a PE thin film, i.e. for the LPG with $(PE\text{-}CNT)_{10}$ thin film, the transmission intensity of the two resonance wavelengths (a sensitivity about -0.17 dB/pH at λ_{res} = 1502 nm and a sensitivity of about -0.83 dB/pH at λ_{res} = 1548 nm) increases with the increasing pH ranging from 2 to 13 (refer to Figs. 8(a) and (b)). From the RI sensing results, it can be obtained that the RI of the $(PE\text{-}CNT)_{10}$ thin film decreases with an increase of pH. This behavior is explained by the pH-dependent thickness and surface topology of $(PE\text{-}CNT)_{10}$ thin films [40,41]. A higher pH would reduce the degree of ionization of one of the weak polyelectrolytes and thus increase the thin film thickness (i.e. decreasing the thin film RI) due to changes in the conformation of polyelectrolyte chains from flat coils to looped structures [41]. The low pH sensitivity for the LPG with $(PE)_{10}$ thin film is due to a small number of bilayers and negligible pH-dependent thickness variations. This result indicates that the LPG with $(PE\text{-}CNT)_{10}$ thin film has an enhanced sensitivity in comparison with a LPG with $(PE)_{10}$ thin film. However, the dynamic response to pH changes of the sensor still needs to be investigated for obtaining an understanding of its reliability and long-term performance and its potentiality for practical applications.

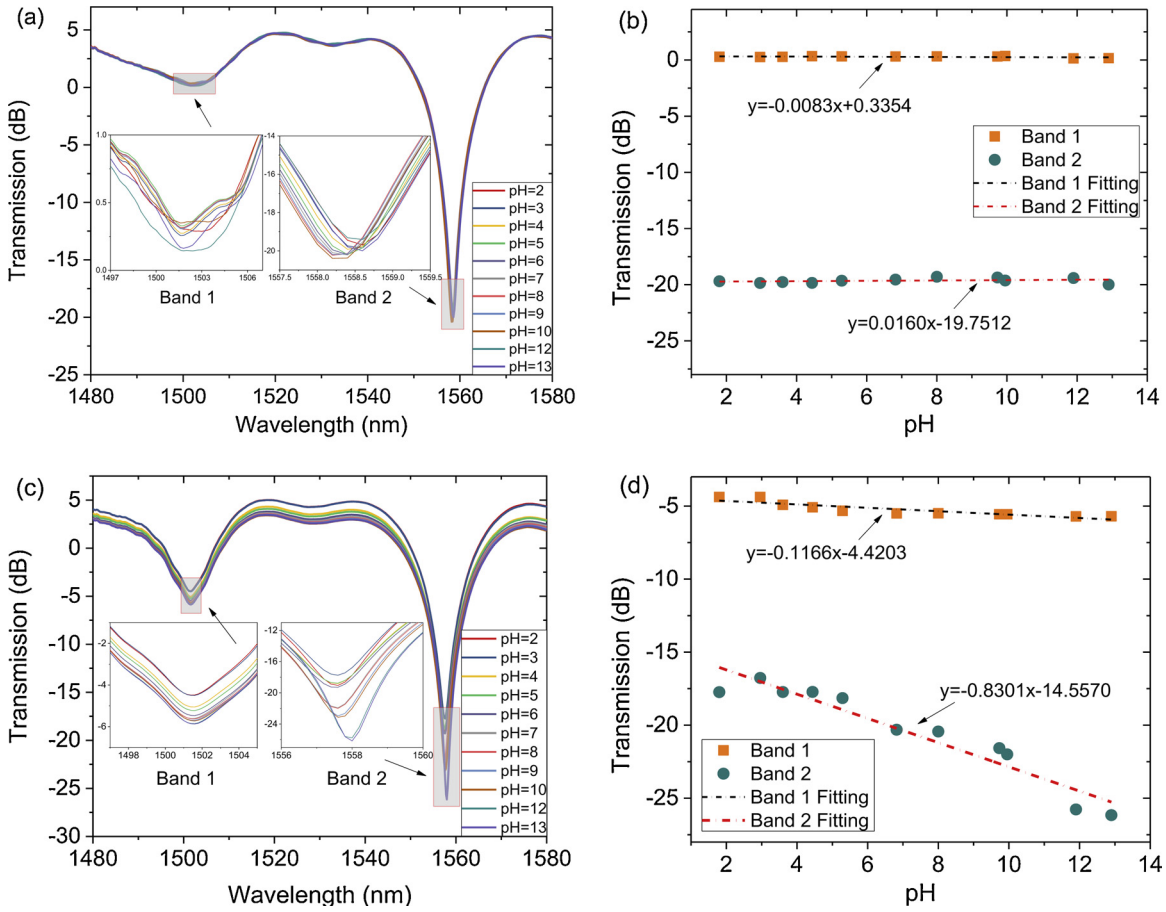

Fig. 8. (a) and (b) Response of the LPG with $(PE)_{10}$ thin film in aqueous pH buffers with different pH ranging from 2 to 13; (c) and (d) Response of the LPG with $(PE\text{-}CNT)_{10}$ thin film in aqueous pH buffers with different pH values ranging from 2 to 13 (Band 1: λ_{res} = 1502 nm; Band 2: λ_{res} = 1548 nm).

4. Conclusions

We successfully employed the LBL assembly technique to deposit an MWCNTs-based nanostructured, i.e. $(PE\text{-}CNT)_{10}$ thin film as a sensing material on a LPG in order to fabricate a novel optical fiber sensor. The wrapping of polyelectrolyte molecules on MWCNT surfaces improves the adhesion of a $(PE\text{-}CNT)_{10}$ thin film onto the LPG grating surface, thus leading to an enhanced performance in terms of sensor sensitivity and durability. In addition, the $(PE\text{-}CNT)_{10}$ with rough and porous morphology results in a sensor with fast response due to the variations of the external refractive index and pH. Such a sensor presents noticeable resonance intensity changes and no wavelength shift over a range of refractive index and pH values, which performs differently from a LPG sensor coated with $(PE)_{10}$ thin film and results in the advantage of achieving an intensity demodulation. This work provides an approach for integration of various nanostructured materials onto optical fiber sensors to form tunable structures and functions for selective sensing applications. Further works will focus on achieving the optimal thickness and refractive index of the PE-CNT thin film to enhance the sensor sensitivity and an understanding of the reliance of the sensing performance on the MWCNT content within a thin film. The effect of the LPG configuration (e.g. grating period, cladding thickness, and grating length) on the sensor sensitivity will also be investigated.

Acknowledgments

The work described in this paper was partially supported by a grant (TRS) from the Research Grants Council of the Hong Kong Special Administrative Region, China (Project No. T22/502/18) and in part by a grant from The Hong Kong Polytechnic University (Project No. 1-BBAG). The authors would also like to appreciate the funding support by the Innovation and Technology Commission of the Hong Kong SAR Government (Project No. K-BBY1).

References

[1] X. Shi, N. Xie, K. Fortune, J. Gong, Durability of steel reinforced concrete in chloride environments: An overview, Constr. Build. Mater. 30 (2012) 125–138.
[2] T.H. Nguyen, T. Venugopala, S. Chen, T. Sun, K.T. Grattan, S.E. Taylor, P.M. Basheer, A.E. Long, Fluorescence based fibre optic pH sensor for the pH 10-13 range suitable for corrosion monitoring in concrete structures, Sens. Actuators B Chem. 191 (2014) 498–507.
[3] J. Wang, J. Tang, Feasibility of fiber Bragg grating and long-period fiber grating sensors under different environmental conditions, Sensors 10 (11) (2010) 10105–10127.
[4] A.M. Vengsarkar, P.J. Lemaire, J.B. Judkins, V. Bhatia, T. Erdogan, J.E. Sipe, Long-period fiber gratings as band-rejection filters, J. Light. Technol. 14 (1) (1996) 58–65.
[5] T. Erdogan, Cladding-mode resonances in short-and long-period fiber grating filters, J. Opt, Soc. Am. A 14 (8) (1997) 1760–1773.
[6] H.J. Patrick, A.D. Kersey, F. Bucholtz, Analysis of the response of long period fiber gratings to external index of refraction, J. Light. Technol. 16 (9) (1998) 1606–1612.
[7] I. Del Villar, I.R. Matías, F.J. Arregui, P. Lalanne, Optimization of sensitivity in long period fiber gratings with overlay deposition, Opt. Express 13 (1) (2005) 56–69.
[8] S.W. James, R.P. Tatam, Fibre optic sensors with nano-structured coatings, J. Opt. A. Pure Appl. Opt. 8 (7) (2006) 430–444.
[9] R.H. Baughman, A.A. Zakhidov, W.A. De Heer, Carbon nanotubes-the route toward applications, Science 297 (5582) (2002) 787–792.
[10] M. Penza, G. Cassano, P. Aversa, F. Antolini, A. Cusano, A. Cutolo, M. Giordano, L. Nicolais, Alcohol detection using carbon nanotubes acoustic and optical sensors, Appl. Phys. Lett. 85 (12) (2004) 2379–2381.
[11] M. Consales, A. Crescitelli, M. Penza, P. Aversa, P.D. Veneri, M. Giordano, A. Cusano, SWCNT nano-composite optical sensors for VOC and gas trace detection, Sens. Actuators B Chem. 138 (1) (2009) 351–361.
[12] B.N. Shivananju, S. Yamdagni, R. Fazuldeen, A.S. Kumar, G.M. Hegde, M.M. Varma, S. Asokan, CO_2 sensing at room temperature using carbon nanotubes coated core fiber Bragg grating, Rev. Sci. Instrum. 84 (6) (2013) 065002.

[13] Y.C. Tan, W.B. Ji, V. Mamidala, K.K. Chow, S.C. Tjin, Carbon-nanotube-deposited long period fiber grating for continuous refractive index sensor applications, Sens. Actuators B Chem. 196 (2014) 260–264.
[14] S.Y. Set, H. Yaguchi, Y. Tanaka, M. Jablonski, Laser mode locking using a saturable absorber incorporating carbon nanotubes, J. Light. Technol. 22 (1) (2004) 51–56.
[15] B. Jiang, M. Xue, C. Zhao, D. Mao, K. Zhou, L. Zhang, J. Zhao, Refractometer probe based on a reflective carbon nanotube-modified microfiber Bragg grating, Appl. Opt. 55 (25) (2016) 7037–7041.
[16] A.A. Badmos, Q. Sun, Z. Yan, R.N. Arif, J. Zhang, A. Rozhin, L. Zhang, High-sensitivity refractive index sensor based on large-angle tilted fiber grating with carbon nanotube deposition, Proc. SPIE. Int. Soc. Opt. Eng. (2016) 989916.
[17] Y. Wang, J.T. Yeow, A review of carbon nanotubes-based gas sensors, J. Sens. 2009 (2009) 493904.
[18] C.R. Zamarreno, I.R. Matias, F.J. Arregui, Nanofabrication techniques applied to the development of novel optical fiber sensors based on nanostructured coatings, IEEE Sens. J. 12 (8) (2012) 2699–2710.
[19] V.H. Pham, T.V. Cuong, S.H. Hur, E.W. Shin, J.S. Kim, J.S. Chung, E.J. Kim, Fast and simple fabrication of a large transparent chemically-converted graphene film by spray-coating, Carbon 48 (7) (2010) 1945–1951.
[20] J. Zasadzinski, R. Viswanathan, L. Madsen, J. Garnaes, D. Schwartz, Langmuir-blodgett films, Science 263 (5154) (1994) 1726–1738.
[21] G. Decher, J.B. Schlenoff, Multilayer Thin Films: Sequential Assembly of Nanocomposite Materials, 2nd ed., John Wiley & Sons, 2006.
[22] T. Lee, S.H. Min, M. Gu, Y.K. Jung, W. Lee, J.U. Lee, D.G. Seong, B.-S. Kim, Layer-by-layer assembly for graphene-based multilayer nanocomposites: synthesis and applications, Chem. Mater. 27 (11) (2015) 3785–3796.
[23] A. Urrutia, J. Goicoechea, A.L. Ricchiuti, D. Barrera, S. Sales, F.J. Arregui, Simultaneous measurement of humidity and temperature based on a partially coated optical fiber long period grating, Sens. Actuators B Chem. 227 (2016) 135–141.
[24] S. Zheng, Long-period fiber grating moisture sensor with nano-structured coatings for structural health monitoring, Struct. Health. Monit. 14 (2) (2015) 148–157.
[25] M. Yin, B. Huang, S. Gao, A. Zhang, X. Ye, Optical fiber LPG biosensor integrated microfluidic chip for ultrasensitive glucose detection, Biomed. Opt. Express 7 (5) (2016) 2067–2077.
[26] M. Yin, C. Wu, L. Shao, W.K.E. Chan, A. Zhang, C. Lu, H. Tam, Label-free, disposable fiber-optic biosensors for DNA hybridization detection, Analyst. 138 (7) (2013) 1988–1994.
[27] M.J. O'Connell, P. Boul, L.M. Ericson, C. Huffman, Y. Wang, E. Haroz, C. Kuper, J. Tour, K.D. Ausman, R.E. Smalley, Reversible water-solubilization of single-walled carbon nanotubes by polymer wrapping, Chem. Phys. Lett. 342 (3–4) (2001) 265–271.
[28] A. Liu, I. Honma, M. Ichihara, H. Zhou, Poly (acrylic acid)-wrapped multi-walled carbon nanotubes composite solubilization in water: definitive spectroscopic properties, Nanotechnology. 17 (12) (2006) 2845.
[29] M.D. Rubianes, G.A. Rivas, Dispersion of multi-wall carbon nanotubes in polyethylenimine: a new alternative for preparing electrochemical sensors, Electrochem. Commun. 9 (3) (2007) 480–484.
[30] S.W. Kim, T. Kim, Y.S. Kim, H.S. Choi, H.J. Lim, S.J. Yang, C.R. Park, Surface modifications for the effective dispersion of carbon nanotubes in solvents and polymers, Carbon. 50 (1) (2012) 3–33.
[31] J.L. Lutkenhaus, K. McEnnis, P.T. Hammond, Nano-and microporous layer-by-layer assemblies containing linear poly (ethylenimine) and poly (acrylic acid), Macromolecules. 41 (16) (2008) 6047–6054.
[32] Y. Li, T. Wu, M. Yang, Humidity sensors based on the composite of multi-walled carbon nanotubes and crosslinked polyelectrolyte with good sensitivity and capability of detecting low humidity, Sens. Actuators B Chem. 203 (2014) 63–70.
[33] Q. Zhao, M. Yin, A.P. Zhang, S. Prescher, M. Antonietti, J. Yuan, Hierarchically structured nanoporous poly (ionic liquid) membranes: facile preparation and application in fiber-optic pH sensing, J. Am. Chem. Soc. 135 (15) (2013) 5549–5552.
[34] R. Yang, W. Dong, X. Meng, X. Zhang, Y. Sun, Y. Hao, J. Guo, W. Zhang, Y. Yu, J. Song, Z. Qi, H. Sun, Nanoporous TiO_2/polyion thin-film-coated long-period grating sensors for the direct measurement of low-molecular-weight analytes, Langmuir. 28 (23) (2012) 8814–8821.
[35] D.B. Stegall, T. Erdogan, Leaky cladding mode propagation in long-period fiber grating devices, IEEE Photonics Technol. Lett. 11 (3) (1999) 343–345.
[36] A. Singh, S.B. Rana, M. Singh, A. Sharma, Study and investigation of long period grating as refractive index sensor, Optik. 125 (7) (2014) 1860–1863.
[37] C. Guan, X. Tian, S. Li, X. Zhong, J. Shi, L. Yuan, Long period fiber grating and high sensitivity refractive index sensor based on hollow eccentric optical fiber, Sens. Actuators B Chem. 188 (2013) 768–771.
[38] C.R. Zamarreño, J. Bravo, J. Goicoechea, I.R. Matias, F.J. Arregui, Response time enhancement of pH sensing films by means of hydrophilic nanostructured coatings, Sens. Actuators B Chem. 128 (1) (2007) 138–144.
[39] C.R. Zamarreño, M. Hernáez, I. Del Villar, I.R. Matías, F.J. Arregui, Optical fiber pH sensor based on lossy-mode resonances by means of thin polymeric coatings, Sens. Actuators B Chem. 155 (1) (2011) 290–297.
[40] J.M. Corres, I.R. Matias, I. Del Villar, F.J. Arregui, Design of pH sensors in long-period fiber gratings using polymeric nanocoatings, IEEE Sens. J. 7 (3) (2007) 455–463.
[41] S.W. Lee, B.S. Kim, S. Chen, Y. Shao-Horn, P.T. Hammond, Layer-by-layer assembly of all carbon nanotube ultrathin films for electrochemical applications, J. Am. Chem. Soc. 131 (2) (2008) 671–679.

Yi-QingNi received his Bachelor degree (1983) and Master degree (1986) from Zhejiang University, China and his PhD degree (1997) from The Hong Kong Polytechnic University, Hong Kong. He is currently a Chair Professor of Smart Structures and Rail Transit at Department of Civil and Environmental Engineering, The Hong Kong Polytechnic University, Hong Kong. He also serves as the Director of the National Engineering Research Center on Rail Transit Electrification and Automation at The Hong Kong Polytechnic University, Hong Kong. His research areas cover structural health monitoring, smart materials and structures, and sensors and actuators.

Siqi Ding received his Bachelor degree (2013) in Material Science and Technology from Dalian Jiaotong University, China and Master degree (2015) in Material Science from Dalian University of Technology, China. He is currently a PhD candidate at The Hong Kong Polytechnic University, Hong Kong. His research focuses on smart materials and structures, nanotechnology, and structural health monitoring.

Baoguo Han received his Bachelor degree (1999), Master degree (2001) and PhD degree (2005) from Harbin Institute of Technology, China. He is currently a Professor at School of Civil Engineering, Dalian University of Technology, China. His research interests include multifunctional/smart materials and structures, high-performance concrete and structures, nanotechnology in civil engineering, and structural health monitoring and traffic detection.

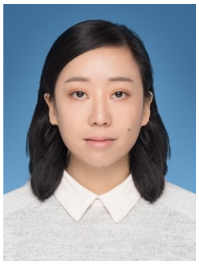

Huaping Wang received her Bachelor degree (2007) and Master degree (2009) from Wuhan University of Technology, China and her PhD degree (2015) from Dalian University of Technology, China. She was a visiting scholar at The Hong Kong Polytechnic University between 2015 and 2017. She is currently an Associate Professor at School of Civil Engineering and Mechanics, Lanzhou University, China. Her research interests include structural health monitoring, optical fiber-based sensing technology, damage identification, and condition assessment.